

# The MAJORANA Neutrinoless Double-Beta Decay Experiment

V.E. Guiseppe<sup>12</sup>, C.E. Aalseth<sup>17</sup>, M. Akashi-Ronquest<sup>13,22</sup>, M. Amman<sup>9</sup>, J.F. Amsbaugh<sup>23</sup>, F.T. Avignone III<sup>19,15</sup>, H.O. Back<sup>14,22</sup>, A.S. Barabash<sup>7</sup>, P. Barbeau<sup>5</sup>, J.R. Beene<sup>15</sup>, M. Bergevin<sup>11</sup>, F.E. Bertrand<sup>15</sup>, M. Boswell<sup>13,22</sup>, V. Brudanin<sup>8</sup>, W. Bugg<sup>21</sup>, T.H. Burritt<sup>23</sup>, Y-D. Chan<sup>11</sup>, T.V. Cianciolo<sup>15</sup>, J. Collar<sup>5</sup>, R. Creswick<sup>19</sup>, M. Cromaz<sup>11</sup>, J.A. Detwiler<sup>11</sup>, P.J. Doe<sup>23</sup>, J.A. Dunmore<sup>23</sup>, Yu. Efremenko<sup>21</sup>, V. Egorov<sup>8</sup>, H. Ejiri<sup>16</sup>, S.R. Elliott<sup>12</sup>, J. Ely<sup>17</sup>, J. Esterline<sup>6,22</sup>, H. Farach<sup>19</sup>, T. Farmer<sup>17</sup>, J. Fast<sup>17</sup>, P. Finnerty<sup>13,22</sup>, B. Fujikawa<sup>11</sup>, V.M. Gehman<sup>12</sup>, C. Greenberg<sup>5</sup>, K. Gusev<sup>8</sup>, A.L. Hallin<sup>1</sup>, R. Hazama<sup>16</sup>, R. Henning<sup>13,22</sup>, A. Hime<sup>12</sup>, E. Hoppe<sup>17</sup>, T. Hossbach<sup>19,17</sup>, M.A. Howe<sup>13,22</sup>, D. Hurley<sup>11</sup>, B. Hyronimus<sup>17</sup>, R.A. Johnson<sup>23</sup>, K.J. Keeter<sup>2</sup>, M. Keillor<sup>17</sup>, C. Keller<sup>20</sup>, J. Kephart<sup>14,22,17</sup>, M. Kidd<sup>6,22</sup>, O. Kochetov<sup>8</sup>, S.I. Konovalov<sup>7</sup>, R.T. Kouzes<sup>17</sup>, K.T. Lesko<sup>10,4</sup>, L. Leviner<sup>14,22</sup>, P. Luke<sup>9</sup>, A.B. McDonald<sup>18</sup>, S. MacMullin<sup>13,22</sup>, M.G. Marino<sup>23</sup>, D.-M. Mei<sup>20</sup>, H.S. Miley<sup>17</sup>, A.W. Myers<sup>23</sup>, M. Nomachi<sup>16</sup>, B. Odom<sup>5</sup>, J. Orrell<sup>17</sup>, A.W.P. Poon<sup>11</sup>, G. Prior<sup>11</sup>, D.C. Radford<sup>15</sup>, J.H. Reeves<sup>17</sup>, K. Rielage<sup>12</sup>, N. Riley<sup>5</sup>, R.G.H. Robertson<sup>23</sup>, L. Rodriguez<sup>12</sup>, K.P. Rykaczewski<sup>15</sup>, A.G. Schubert<sup>23</sup>, T. Shima<sup>16</sup>, M. Shirchenko<sup>8</sup>, J. Strain<sup>13,22</sup>, R. Thompson<sup>17</sup>, V. Timkin<sup>8</sup>, W. Tornow<sup>6,22</sup>, C. Tull<sup>11</sup>, T. D. Van Wechel<sup>23</sup>, I. Vanyushin<sup>7</sup>, R.L. Varner<sup>15</sup>, K. Vetter<sup>11,3</sup>, R. Warner<sup>17</sup>, J.F. Wilkerson<sup>13,22</sup>, J.M. Wouters<sup>12</sup>, E. Yakushev<sup>8</sup>, A.R. Young<sup>14,22</sup>, C.-H. Yu<sup>15</sup>, V. Yumatov<sup>7</sup>, C. Zhang<sup>20</sup>

(MAJORANA Collaboration)

**Abstract**—Neutrinoless double-beta decay searches play a major role in determining the nature of neutrinos, the existence of a lepton violating process, and the effective Majorana neutrino mass. The MAJORANA Collaboration proposes to assemble an array of HPGe detectors to search for neutrinoless double-beta decay in <sup>76</sup>Ge. Our proposed method uses the well-established technique of searching for neutrinoless double-beta decay in high purity Ge-diode radiation detectors that play both roles

of source and detector. The technique is augmented with recent improvements in signal processing and detector design, and advances in controlling intrinsic and external backgrounds. Initially, MAJORANA aims to construct a prototype module containing 60 kg of Ge detectors to demonstrate the potential of a future 1-tonne experiment. The design and potential reach of this prototype Demonstrator module will be presented. This paper will also discuss detector optimization and low-background requirements, such as material purity, background rejection, and identification of rare backgrounds required to reach the sensitivity goals of the MAJORANA experiment.

## I. INTRODUCTION

WITH the realization that neutrinos are not massless particles, but have mass and mix, there is increased interest in investigating their intrinsic properties. Understanding the neutrino mass generation mechanism, the absolute neutrino mass scale and the neutrino mass spectrum are some of the main focuses of future neutrino experiments. The discovery of Majorana neutrinos would have profound theoretical implications in the formation of a new Standard Model while yielding insights into the origin of mass itself. As of yet, there is no firm experimental evidence to confirm or refute this theoretical prejudice. Experimental evidence of neutrinoless double-beta ( $0\nu\beta\beta$ ) decay would definitively establish the Majorana nature of neutrinos. Not only is  $0\nu\beta\beta$  decay the only practical method to uncover the Majorana nature of neutrinos, it has the potential to reach an absolute mass scale sensitivity of  $<50$  meV. Observation of a sharp peak at the  $\beta\beta$  endpoint would quantify the  $0\nu\beta\beta$ -decay rate, demonstrate that neutrinos are Majorana particles, indicate that lepton number is not conserved, and provide a measure of the effective Majorana mass of the electron neutrino [1]–[6].

<sup>1</sup> Centre for Particle Phys., Univ. of Alberta, Edmonton, Alberta, Canada  
<sup>2</sup> Department of Physics, Black Hills State University, Spearhead, SD, USA  
<sup>3</sup> Department of Nuclear Engineering, UC Berkeley, Berkeley, CA, USA  
<sup>4</sup> Department of Physics, UC Berkeley, Berkeley, CA, USA  
<sup>5</sup> University of Chicago, Chicago, IL, USA  
<sup>6</sup> Department of Physics, Duke University, Durham, NC, USA  
<sup>7</sup> Institute for Theoretical and Experimental Physics, Moscow, Russia  
<sup>8</sup> Joint Institute for Nuclear Research, Dubna, Russia  
<sup>9</sup> Engineering Div., Lawrence Berkeley Natl. Lab., Berkeley, CA, USA  
<sup>10</sup> Inst. for Nucl. & Part. Astro., Lawrence Berkeley Natl. Lab., Berkeley, CA, USA  
<sup>11</sup> Nuclear Science Div., Lawrence Berkeley Natl. Lab., Berkeley, CA, USA  
<sup>12</sup> Physics Div., Los Alamos National Laboratory, Los Alamos, NM, USA  
<sup>13</sup> Dept. of Phys. and Astron., Univ. of North Carolina, Chapel Hill, NC, USA  
<sup>14</sup> Department of Physics, North Carolina State Univ., Raleigh, NC, USA  
<sup>15</sup> Oak Ridge National Laboratory, Oak Ridge, TN, USA  
<sup>16</sup> Res. Center for Nucl. Phys. & Dept. of Phys., Osaka Univ., Ibaraki, Osaka, Japan  
<sup>17</sup> Pacific Northwest National Laboratory, Richland, WA, USA  
<sup>18</sup> Dept. of Physics, Queen's University, Kingston, Ontario, Canada  
<sup>19</sup> Dept. of Phys. and Astron., Univ. of South Carolina, Columbia, SC, USA  
<sup>20</sup> Dept. of Earth Science and Phys., Univ. of South Dakota, Vermillion, SD, USA  
<sup>21</sup> Dept. of Physics and Astron., Univ. of Tennessee, Knoxville, TN, USA  
<sup>22</sup> Triangle Universities Nuclear Laboratory, Durham, NC, USA  
<sup>23</sup> Center for Nucl. Phys. and Astrophys., Univ. of Washington, Seattle, WA, USA  
V.E. Guiseppe is with Los Alamos National Laboratory, Los Alamos, NM 87545 USA (e-mail: guiseppe@lanl.gov)

Ordinary beta decay of many heavy even-even nuclei is energetically forbidden or strongly spin inhibited. However, a process in which a nucleus changes its atomic number by two while simultaneously emitting two beta particles is energetically possible for some even-even nuclei. In two-neutrino double-beta decay ( $2\nu\beta\beta$ ), the nucleus emits 2  $\beta$  particles and 2  $\bar{\nu}_e$  conserving lepton number. It is an allowed second-order weak process that occurs in nature, although its rate is extremely low. Half-lives for this decay mode have been measured at  $\sim 10^{19}$  years or longer in several nuclei [7].

The more interesting process is zero-neutrino double-beta decay ( $0\nu\beta\beta$ ) where only the 2  $\beta$  particles are emitted and no neutrinos. Unlike  $2\nu\beta\beta$ ,  $0\nu\beta\beta$  violates lepton number conservation and hence requires physics beyond the Standard Model. One can visualize  $0\nu\beta\beta$  as an exchange of a virtual neutrino between two neutrons within the nucleus. In the framework of the  $SU_L(2) \times U(1)$  Standard Model of weak interactions, the first neutron emits a right-handed anti-neutrino. However, the second neutron requires the absorption of a left-handed neutrino. In order for this to happen, the neutrino must have mass so that it is not in a pure helicity state, and the neutrino and anti-neutrino have to be indistinguishable. That is, the neutrino would have to be a massive Majorana particle.

One isotope known to undergo  $\beta\beta$ -decay is  $^{76}\text{Ge}$ . The MAJORANA Collaboration has proposed an experiment [8] using the well-established technique of searching for  $0\nu\beta\beta$  decay in high-purity Ge-diode radiation detectors that play both roles of source and detector. The technique maximizes the source to total mass ratio and benefits from excellent energy resolution (0.16% at 2.039 MeV). Ge detectors are able to be enriched in the  $\beta\beta$ -decay isotope  $^{76}\text{Ge}$  from 7.44% to 86%. Ge-based  $0\nu\beta\beta$  experiments have established the best half-life limits and the most restrictive constraints on the effective Majorana mass for the neutrino [9], [10]. One analysis of the data in Ref. [10] claims evidence for  $0\nu\beta\beta$  with a half-life of  $2.23^{+0.44}_{-0.31} \times 10^{25}$  y [11].

The future use of Ge detectors can be augmented with recent improvements in signal processing and detector design, and advances in controlling intrinsic and external backgrounds. Progress in signal processing from segmented Ge-diode detectors potentially offers significant benefits in rejecting backgrounds, reducing sensitivity of the experiment to backgrounds, and providing additional handles on both signals and backgrounds through multi-dimensional event reconstruction. Development of sophisticated Cu-electroforming methods allow the fabrication of ultra-low-background materials required for the construction of next-generation experiments.

## II. THE MAJORANA APPROACH

The MAJORANA collaboration is currently pursuing R&D aimed at a 1-tonne scale,  $^{76}\text{Ge}$   $0\nu\beta\beta$ -decay experiment that potentially would be one of the initial suite of experiments to be sited at the U.S. Deep Underground Science and Engineering Laboratory (DUSEL) in the former Homestake Mine in South Dakota [12]. The goals of a 1-tonne experiment would be to determine the Majorana or Dirac nature of neutrinos, test lepton number conservation, and probe the absolute neutrino

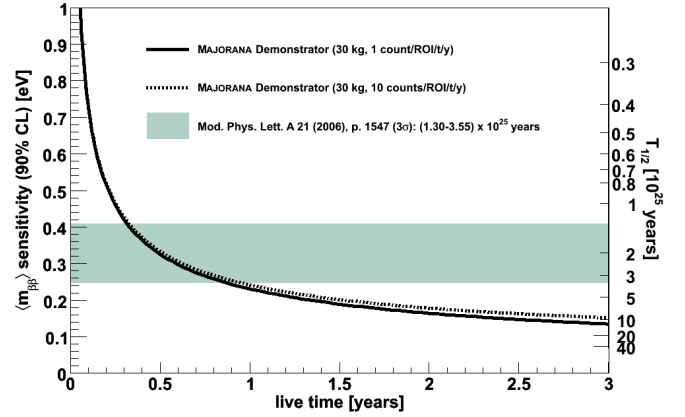


Fig. 1. The  $0\nu\beta\beta$  half-life and effective Majorana mass sensitivity of the MAJORANA Demonstrator module.

mass scale at the atmospheric mass scale of 20-40 meV. We are currently cooperating with the European GERDA Collaboration [13] with the aim to jointly prepare for a single international tonne-scale Ge-based experiment utilizing the best technologies of the two collaborations.

For the R&D phase, the MAJORANA collaboration intends to construct a Demonstrator module of  $^{76}\text{Ge}$  crystals contained in an ultra-low-background structure. The MAJORANA R&D Demonstrator module should significantly improve the lower limits on the decay lifetime from the current level of about  $2 \times 10^{25}$  years to about  $7 \times 10^{26}$  years, corresponding to an upper limit of 90 meV on the effective Majorana electron-neutrino mass (Fig. 1). The Demonstrator module will be located at the 4850-ft level (4200 m.w.e) at the Sanford Laboratory, the future home of DUSEL.

The Demonstrator reference design is a modular concept with three individual cryostats (Fig. 2) containing a combination of enriched (86%-enrichment) and unenriched (natural) Ge crystals. This R&D system allows exploration of segmentation schemes and detector types. Our initial emphasis will be on a first cryostat assembled with natural-Ge P-PC detectors. The modular concept provides timely step-wise installation, access, and future up-scaling. By using 30 kg of 86% enriched  $^{76}\text{Ge}$  crystals, the  $0\nu\beta\beta$  claim [11] will be tested after 2 y of running. The additional 30 kg of natural Ge allows enough total sensitivity to understand backgrounds. The background goal in the  $0\nu\beta\beta$  peak 4-keV region of interest centered at 2039 keV is 1 count/tonne/year after analysis cuts.

The detectors will be mounted in a string-like arrangement as shown in Figure 2. The reference design of the string, which continues to be refined, currently consists of a thick copper “lid”, a copper support frame, and low-mass plastic support trays or stand-offs. Each individual detector is mounted in a separate frame built of electro-formed Cu that eases handling of individual detectors during shipping, acceptance testing and string assembly. The assembled detector string is lowered through a hole in the cryostat cold plate until the string lid sits on the cold plate. This allows us to mount and dismount individual detector strings from the top. Cables are

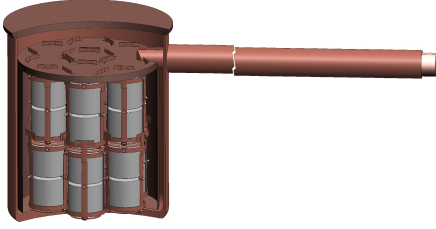


Fig. 2. A representation of the one of three low-mass, low-background cryostat design of the MAJORANA Demonstrator.

run vertically from the detector contacts through a slit in the string lid, above which low-background front-end electronics packages are mounted for reading out the central contact. The string lid provides some shielding between these components and the detectors, and allows the bandwidth to be maximized by placing the central contact FETs near the Ge detectors.

All crystals are enclosed in ultra-pure, electro-formed copper cryostats. A thermal shroud mounted to the cold plate provides radiative cooling for the detector array. The cryostat, cold plate and thermal shroud will be fabricated using ultra-low-background electro-formed copper. This copper is the lowest radioactivity material we will have available and a relatively thick cryostat wall can be used to make a strong vacuum vessel. See Section III for more details on the electro-forming process.

The cryostats will be enclosed in a graded passive shield (Fig. 3) and an active muon veto to eliminate external backgrounds. Shielding reduces signals from  $\gamma$  rays originating in the experiment hall (from rock, construction materials, and from the shielding materials themselves), cosmic-ray  $\mu$ 's penetrating the shielding, and cosmic-ray  $\mu$ -induced neutrons. The strategy is to provide extremely low-activity material for the *inner shield*. Surrounding this will be an *outer shield* of bulk  $\gamma$ -ray shielding material with lower radiopurity. This high- $Z$  shielding enclosure will be contained inside a gas-tight Rn exclusion box made of stainless-steel sheet. Outside this bulk high- $Z$  shielding will be a layer of hydrogenous material, some of which will be doped with a neutron absorber such as boron, intended to reduce the neutron flux. Finally, active cosmic-ray anti-coincidence detectors will enclose the entire shield.

Monte Carlo (MC) radiation transport simulation models have been developed for MAJORANA using MaGe [14], an object-oriented MC simulation package based on ROOT [15] and the Geant4 [16], [17] toolkit. MaGe is optimized for simulations of low-background Ge detector arrays and is being jointly developed by the MAJORANA and GERDA [13] collaborations. MaGe defines a set of physics processes, materials, constants, event generators, etc. that are common to these experiments, and provides a unified framework for geometrical definitions, database access, user interfaces, and simulation output schemes in an effort to reduce repetition of labor and increase code scrutiny.

Typical HPGe digitization electronics entail a digitizing

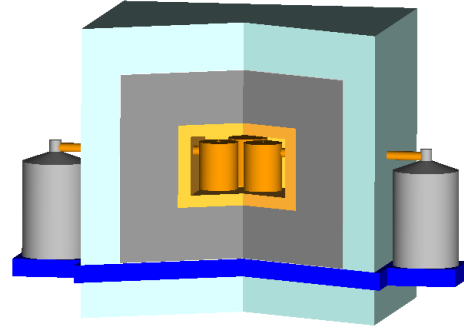


Fig. 3. A representation of the passive shield for the MAJORANA Demonstrator. Shown are three cryostats surrounding by Cu, Pb, and neutron moderating passive shielding layers.

ADC read out by an on-board FPGA. Such a card has been custom-designed to readout the GRETINA detectors [18]. Such a board is well-matched to the digital signal processing needs of MAJORANA. The DAQ software system will be constructed using the Object-oriented Real-time Control and Acquisition (ORCA) [19] application which provides a general purpose, highly modular, object-oriented, acquisition and control system that is easy to develop, use, and maintain. With the ability to control embedded single board computers, ORCA extends its ease of use to a wide range of hardware options [20].

### III. BACKGROUNDS

Mitigation of backgrounds is crucial to the success of any rare decay search. For the case of Ge solid-state detectors, decades of research have yielded a host of techniques to reduce backgrounds. These techniques include the use of ultra-pure materials for the construction of detector components in the proximity of the crystals, shielding the detectors from external natural and cosmogenic sources, and optimizing detector energy resolution to enhance the spectral information available. The key to the MAJORANA design is the ability to reduce backgrounds to unprecedented levels.

Typical backgrounds that require mitigation include the natural radioactive chains, anthropogenic isotopes, and cosmogenics. The isotopes produced by cosmic activation are particularly problematic. At the Earth's surface, cosmic rays can activate isotopes in detector materials. These backgrounds will be reduced by carefully limiting exposure of detector and susceptible shielding materials above ground. As much production as possible will take place underground. Once underground, backgrounds can be produced from the remaining muon-induced hard, secondary neutrons interacting in the detector and shielding materials. The detector shielding will utilize neutron moderating material and an active muon veto to limit this class of background.

Copper is one of the very few elements having no relatively long-lived radioisotopes. It also has excellent physical, chemical, and electronic properties that make it particularly useful in the fabrication of low-background radiation detectors. Nevertheless, one must take care to ensure that it is not contaminated with radioactive impurities, and that it does not have

significant quantities of cosmic ray generated radioisotopes. The most serious of these latter impurities is  $^{60}\text{Co}$ , which is generated by  $(n,\alpha)$  reactions on  $^{63}\text{Cu}$ . Ultra-pure copper for use in MAJORANA will be produced by an electro-forming process underground.

The electro-forming process [21] uses an acidic  $\text{CuSO}_4$  solution through which positive copper ions are induced from a copper anode to a stainless steel mandrel which initially serves as the cathode. The sacrificial copper anode material is consumed and replaced as necessary as the electro-formed part is formed at the cathode. Highest purity copper is obtained by carefully limiting the electro-forming potential to selectively eliminate a wide variety of contaminants that reside in the bath as the less pure anode copper source material is consumed. Optimal material is achieved by controlling the rate of plating (i.e. current density at the Cu surface), manipulation of electrode surface boundary layers (via agitation, reverse pulse plating, etc.), and the use of crystal growth inhibiting chemicals. The optimization of electro-forming copper with adequate structural integrity and high purity is underway.

Copper cleanliness studies have shown that the  $\text{CuSO}_4$  in the bath is the source of Th in the produced copper parts. Producing  $\text{CuSO}_4$  from pure starting materials has been more successful in producing clean copper parts than re-crystallizing the  $\text{CuSO}_4$ .

Recent advances have provided new background-rejection techniques in the form of pulse-shape analysis, detector segmentation, and granularity (inter-detector coincidences). These techniques rely on the different spatial distributions of energy deposition between double-beta decay events and most background signals. Background signals arising from radioactive decay often include a beta and one or more  $\gamma$  rays. In addition, a 2-MeV  $\gamma$  ray frequently undergoes multiple scatters on the centimeter scale. Double-beta decay energy deposition occurs within a small volume ( $<1\text{ mm}^3$ ) and hence is single site.

The pulse-shape analysis makes use of a digitized preamplifier pulse shape to extract key pulse parameters, including the width, asymmetry, kurtosis, and higher moments. Analysis of these parameters indicate whether an event is single- or multi-site. Electrically subdividing the detector into smaller elements gives additional segmentation discrimination between single site events like  $0\nu\beta\beta$  decay and internal or external  $\gamma$ -ray backgrounds. In a closely packed array of detectors, there is a large probability for hits in multiple detectors from internally generated  $\gamma$  rays that escape a crystal, Compton scatter  $\gamma$  rays from external sources, and traversing muons. The appearance of hits in several nearby detectors within a short (few microsecond) coincidence window provides a large-scale multiplicity or granularity cut. Single-site, time-correlated (SSTC) cuts are decay-chain-specific. This method looks forward or backwards in time from an event in the ROI to find signatures of parent or daughter isotopes [5]. Given a raw event rate of roughly 1 event per crystal per day, this method will work exceptionally well for internal, short-lived parent-daughter pairs like  $^{68}\text{Ge}$ - $^{68}\text{Ga}$  and for decays of internal contaminants, with somewhat lower rejection efficiency. It will also play an important role in diagnosing and eliminating surface contamination of U and Th chain isotopes.

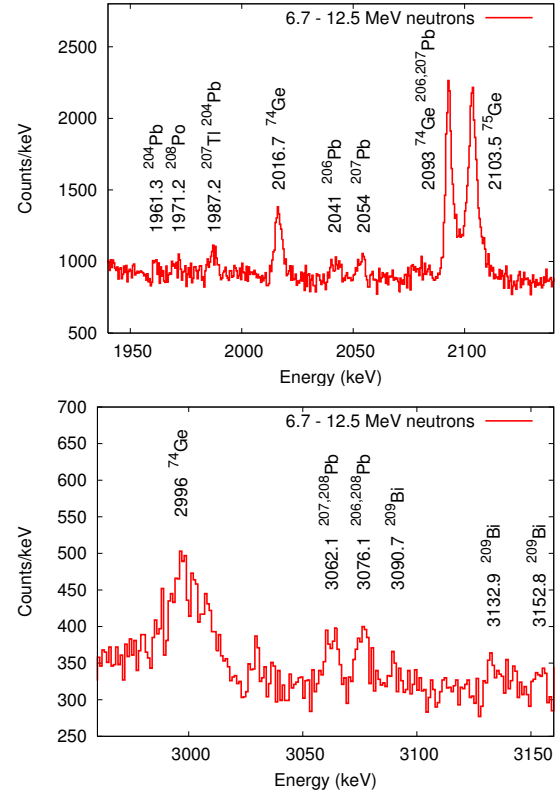


Fig. 4. The  $\gamma$ -ray spectra showing the 2041-keV  $\gamma$ -ray line and the 3062-keV  $\gamma$ -ray line from 6.7-12.5 MeV neutrons [22].

If the efforts to reduce the natural decay chain isotopes are successful, previously unimportant components of the background must be understood and eliminated. For example,  $(n,n'\gamma)$  reactions will become important for tonne-scale double-beta decay experiments [23]. Specific Pb  $\gamma$ -rays are problematic backgrounds for Ge-based experiments using large quantities of Pb shielding:  $^{206}\text{Pb}$  has a 2040-keV  $\gamma$  ray,  $^{207}\text{Pb}$  has a 3062-keV  $\gamma$  ray, and  $^{208}\text{Pb}$  has a 3060-keV  $\gamma$  ray. The first  $\gamma$  ray is near the  $^{76}\text{Ge}$   $\beta\beta$  Q-value of 2039 keV. The double escape peak of the latter two is a single-site energy deposit near the  $\beta\beta$  Q-value. The levels that produce these  $\gamma$  rays can be excited by  $(n,n'\gamma)$  or  $(n,xn\gamma)$  reactions, but the cross sections are small and previously unmeasured. Excitation of these levels (Fig. 4) were studied with a broad-energy neutron beam to measure reaction cross sections [22]. The cross sections can be folded with the underground neutron flux to estimate background rates.

#### IV. DETECTORS

We are exploring two Ge detector technologies. The first are novel point-contact, p-type (P-PC) detectors (Fig. 5), which have an excellent interaction separation capability, superior energy resolution and low energy threshold. This is due to the point contact's small capacitance and the rapidly changing electrical weighting field in the vicinity of the readout contact. This approach provides a very effective active background separation by pulse-shape analysis with only one readout channel and therefore minimum amount of potentially radioactive

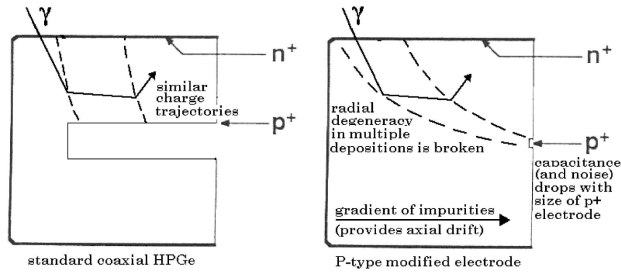


Fig. 5. Closed-end coaxial p-type Ge detector (left) versus the P-PC Ge detector implementation (right) [24].

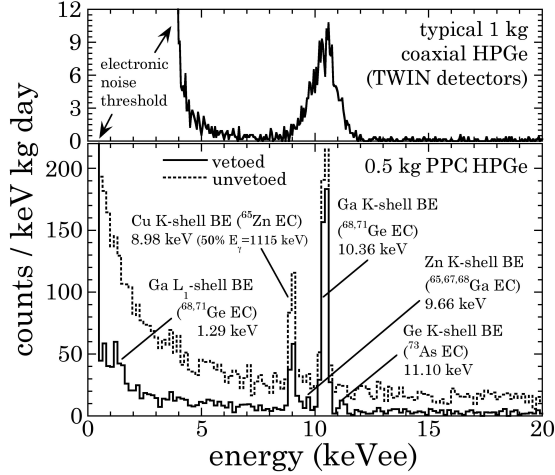


Fig. 6. A demonstration of the improved energy resolution and threshold for P-PC detectors versus a typical coaxial HPGe detector [26].

materials, particularly close to the detector.

The P-PC is an alternative right circular cylindrical detector design developed in which the bore hole is removed and replaced with a point-contact, either implanted B or drifted Li, in the center of the passivated detector face [25]. The changes in the electrode structure result in a drop in capacitance to  $\sim 1$  pF, reducing the electronics noise component and enabling sub-keV energy thresholds. This P-PC configuration also has lower electric fields throughout the bulk of the crystal and a weighting potential that is sharply peaked near the point contact. This in turn results in an increased range of drift times and a distinct electric signal marking the arrival of the charge cloud at the central electrode. Figure 5 illustrates the point-contact implementation in contrast to the conventional, closed-end coaxial detector approach. Instrumented with a modern FETs, P-PC detectors have recently been demonstrated by MAJORANA collaborators to provide low noise, resulting in a low energy trigger threshold and excellent energy resolution (Fig. 6), as well as excellent pulse-shape capabilities (Figs. 7 and 8) to distinguish multiple interactions [24].

Beyond background rejection capabilities, P-PC detectors also have potentially increased manufacturing speed, lower cost, simpler construction and data analysis, and decreased thermal load and photon path. It is anticipated that several crystal growers and vendors will potentially be able to provide this type of detector. Handling and characterization of these

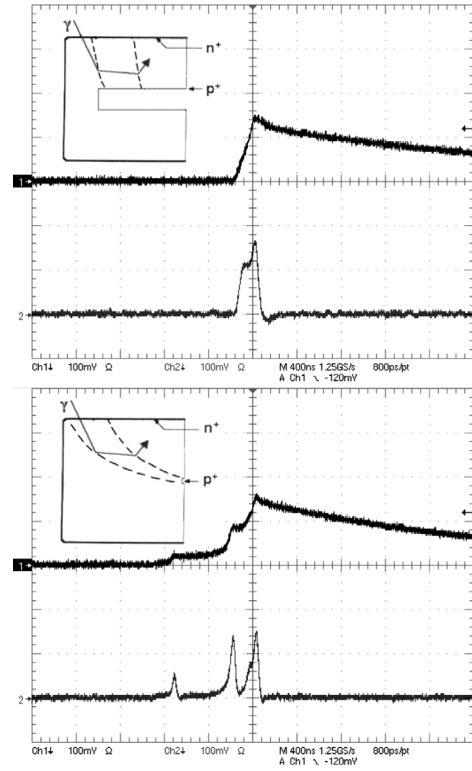


Fig. 7. Pulse shape from closed-end coaxial p-type Ge detector (top) versus the P-PC Ge detector implementation (bottom) [24].

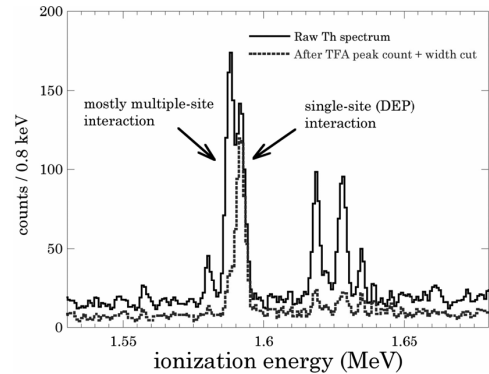


Fig. 8. Pulse shape analysis of a P-PC Ge detector showing the efficiency of rejecting multi-site events (high-energy  $\gamma$  rays) and accepting single-site events (a double escape peak) [24].

detectors is straight forward. Several measures are under study that would reduce surface contamination backgrounds to negligible levels for this type of device: pairing detectors with their passivated ends face-to-face (the only surfaces sensitive to alphas in these devices), and (separately) possibly detecting particle induced x-ray emission from alphas entering one of them.

Until recently, only one operational P-PC detector had been produced, and the chief uncertainty with the P-PC approach was the requirement for the impurity concentration profile in the crystal. During the last year, however, five additional detectors have been produced by three different vendors or institutions (Canberra, Lawrence Berkeley National Laboratory, and PHD's Inc.). In addition to demonstrating that P-



PC detectors are not difficult to produce, the new detectors have validated field calculation codes and simulations that allow us to determine the impurity gradient requirements and the dimensions to which such detectors can reliably be manufactured. This information also enables simulations to design optimal detectors for MAJORANA.

The second detector technology is a segmented detector approach based on large-volume n-type detectors. This approach not only provides the discrimination of single and multiple interactions in three dimensions, it also provides the ability to fully reconstruct individual  $\gamma$  rays by measuring the three-dimensional position (to 2 mm) and energies of each interactions point. Such a capability provides additional information to distinguish the signal from potential backgrounds.

Detectors with a moderate degree of segmentation offer some of the event characterization capability of highly segmented detectors, but with lower complexity, risk, and cost. The segment multiplicity provides an additional handle to separate signal from background over the radial pulse shape analysis and detector granularity techniques of unsegmented p-type detector arrays. In addition, by employing pulse-shape analysis of the segment signals, an improved position sensitivity can be obtained, depending on the number and orientation of the segmentation. Simulations and recent experiments have shown that already with four segments a  $\gamma$  ray of about 2 MeV that leaves its full energy in a detector can be suppressed by a factor of  $\sim 3$  just by employing the segment multiplicity. Employing 40-fold segment multiplicity, the suppression factor only increases to about 5. Compared to non-segmented designs, additional contacts and cables will be required for the segment signals, increasing the risk of extra background sources close to the detectors.

The Segmented Enriched-Germanium Assembly (SEGA) prototype detector is a 12-segment n-type Ge detector enriched to 86% in  $^{76}\text{Ge}$ . It has been used for segmentations studies and pulse-shape analysis techniques. Work is underway to re-mount the crystal in a low background cryostat to study backgrounds. The detector will be operated underground.

## V. CONCLUSION

MAJORANA is conducting R&D for a 1-tonne  $0\nu\beta\beta$  decay experiment by constructing a Demonstrator module of  $^{76}\text{Ge}$  crystals contained in an ultra-low-background structure. Our current Demonstrator reference design is a modular concept with three individual cryostats containing a combination of 30 kg of enriched (86%-enrichment) and 30 kg of unenriched (natural) Ge crystals. This amount of material should demonstrate that the backgrounds are low enough to justify scaling to 1-tonne, as well as probing the neutrino effective mass region above 100 meV.

## ACKNOWLEDGMENT

Preparation of this paper was supported by the U.S. DOE Office of Nuclear Science, the Los Alamos Laboratory Directed Research and Development, and the U.S. NSF Particle and Nuclear Astrophysics.

## REFERENCES

- [1] S. R. Elliott and P. Vogel, "Double beta decay," *Ann. Rev. Nucl. Part. Sci.*, vol. 52, p. 115, 2002.
- [2] S. R. Elliott and J. Engel, "Double-beta decay," *J. Phys. G: Nucl. Part. Phys.*, vol. 30, no. 9, pp. R183–R215, 2004.
- [3] A. S. Barabash, "Double-Beta-Decay Experiments: Present Status and Prospects for the Future," *Physics of Atomic Nuclei*, vol. 67, pp. 438–452, Mar. 2004.
- [4] F. T. Avignone III, G. S. King III, and Y. Zdesenko, "Next generation double-beta decay experiments: Metrics for their evaluation," *New Journal of Physics*, vol. 7, p. 6, 2005.
- [5] H. Ejiri, "Double beta decays and neutrino masses," *J. Phys. Soc. Jap.*, vol. 74, pp. 2101–2127, 2005.
- [6] F. T. Avignone III, S. R. Elliott, and J. Engel, "Double beta decay, Majorana neutrinos, and neutrino mass," *Rev. Mod. Phys.*, vol. 80, pp. 481–516, 2008.
- [7] A. Barabash, "Average and recommended half-life values for two neutrino double beta decay: Upgrade '05," *Czech. J. Phys.*, vol. 56, p. 437, 2006.
- [8] S. R. Elliott *et al.*, "The Majorana Project," 2008. arXiv:0807.1741 [nucl-ex].
- [9] C. E. Aalseth *et al.*, "IGEX  $^{76}\text{Ge}$  neutrinoless double-beta decay experiment: Prospects for next generation experiments," *Phys. Rev. D*, vol. 65, no. 9, p. 092007, 2002.
- [10] L. Baudis *et al.*, "Limits on the Majorana mass in the 0.1 eV range," *Phys. Rev. Lett.*, vol. 83, pp. 41–44, 1999.
- [11] H. V. Klapdor-Kleingrothaus and I. V. Krivosheina, "The evidence for the observation of  $0\nu\beta\beta$  decay: The identification of  $0\nu\beta\beta$  events from the full spectra," *Mod. Phys. Lett. A*, vol. 21, no. 20, pp. 1547–1566, 2006.
- [12] <http://www.lbl.gov/nsd/homestake/>.
- [13] S. Schönert *et al.*, "The GERmanium Detector Array (GERDA) for the search of neutrinoless  $\beta\beta$  decays of  $^{76}\text{Ge}$  at LNGS," *Nucl. Phys. Proc. Suppl.*, vol. 145, p. 242, 2005.
- [14] M. Bauer *et al.*, "MaGe: a Monte Carlo framework for the Gerda and Majorana double beta decay experiments," *J. Phys.: Conf. Ser.*, vol. 39, p. 362, 2006.
- [15] R. Brun and F. Rademakers, "Root: An object oriented data analysis framework," *Nuclear Instruments and Methods in Physics Research A*, vol. 389, pp. 81–86, 1997.
- [16] S. Agostinelli *et al.*, "Geant4: A simulation toolkit," *Nuclear Instruments and Methods in Physics Research A*, vol. 506, pp. 250–303, 2003.
- [17] J. Allison *et al.*, "Geant4 developments and applications," *IEEE Transactions on Nuclear Science*, vol. 53, no. 1, pp. 270–278, 2006.
- [18] M. Descovich, I. Y. Lee, P. Fallon, M. Cromaz, A. O. Macchiavelli, D. C. Radford, K. Vetter, R. M. Clark, M. A. Deleplanque, F. S. Stephens, and D. Ward, "In-beam measurement of the position resolution of a highly segmented coaxial germanium detector," *Nuclear Instruments and Methods in Physics Research A*, vol. 553, pp. 535–542, Nov. 2005.
- [19] M. A. Howe, G. A. Cox, P. J. Harvey, F. McGirt, K. Rielage, J. F. Wilkerson, and J. Wouters, "Sudbury Neutrino Observatory neutral current detector acquisition software overview," *IEEE Transactions on Nuclear Science*, vol. 51, pp. 878–883, 2004.
- [20] M. A. Howe, M. G. Marino, and J. F. Wilkerson, "Integration of embedded single board computers into and object-oriented software bus DAQ application," *These Proceedings*, 2008.
- [21] E. W. Hoppe *et al.*, "Cleaning and passivation of copper surfaces to remove surface radioactivity and prevent oxide formation," *Nuclear Instruments and Methods A*, vol. 579, pp. 486–489, 2007.
- [22] V. E. Guiseppe *et al.*, "Neutron inelastic scattering and reactions in natural Pb as a background in neutrinoless double-beta decay experiments," 2008. arXiv:0809.5074 [nucl-ex].
- [23] D.-M. Mei and A. Hime, "Muon-induced background study for underground laboratories," *Phys. Rev. D*, vol. 73, p. 053004, 2006.
- [24] P. S. Barbeau, J. I. Collar, and O. Tench, "Large-mass ultra-low noise germanium detectors: Performance and applications in neutrino and astroparticle physics," *J. Cosmology and Astroparticle Phys.*, vol. 2007, no. 09, p. 009, 2007.
- [25] P. N. Luke, F. S. Goulding, N. W. Madded, and R. H. Pehl, "Low capacitance large volume shaped-field germanium detector," *IEEE Trans. Nuclear Science*, vol. 36, no. 1, p. 926, 1986.
- [26] C. E. Aalseth *et al.*, "Experimental constraints on a dark matter origin for the DAMA annual modulation effect," 2008. arXiv:0807.0879v4 [astro-ph].